Progress In Electromagnetics Research, PIER 81, 149–166, 2008

STENCIL COEFFICIENT COMPUTATIONS FOR THE MULTIRESOLUTION TIME DOMAIN METHOD — A FILTERBANK APPROACH

S. M. Vaitheeswaran and S. V. Narasimhan

Aerospace Electronics and Systems Division
National Aerospace Laboratories
Kodihalli, Banglaore, India

Abstract—Multiresolution Time Domain (MRTD) techniques based on wavelet expansions can be used for adaptive refinement of computations to economize the resources in regions of space and time where the fields or circuit parameters or their derivatives are large. Hitherto, standard wavelets filter coefficients have been used with the MRTD method but the design of such filter itself may enable to incorporate desired properties for different applications. Towards this, in this paper, a new set of stencil coefficients in terms of scaling coefficients starting from a half band filter, designed by window method and deriving a physically realizable filter by spectral factorization using cepstral technique, for the MRTD method is presented. These stencil coefficients for the MRTD are found to give good agreement with similar MRTD schemes such as those obtained using Daubechies orthogonal wavelets.

1. INTRODUCTION

There is a growing interest in electromagnetic problems of broadband application and in recent times, *time domain* techniques [18] have been widely used for analyzing microwave cavities and circuits [7, 10, 15, 41], electromagnetic scattering applications such as in short-pulse antenna radiation [17, 26–28], high-resolution radar scattering [5, 36], and electromagnetic compatibility [5] and electromagnetic pulse interference problems [1, 2]. Time domain methods have advantages over frequency domain like providing a broadband transient response from a single analysis. Many are applicable for the analysis of time varying or non-linear systems [32]. They easily illustrate the effects at different parts of

the computational domain the linear space-time relationships between the field components that exists in the connecting equations. Further, it is also possible to visualize more physically the propagation of electromagnetic waves and their interactions with structures. In certain transient applications, only the early time response is of interest and the methods can be truncated, allowing the use of complete solutions only as long as necessary.

A very popular and effective method in the time domain has been the Finite Difference Time Domain Method (FDTD) [39] of Maxwell's equations. This method, to become a dominant simulation one for electromagnetic problems has undergone many modifications for the last thirty-five years [5, 10–12, 36, 40, 42, 43]. The method involves a time-based leapfrog approach where the updating equations derived from the differential form of Faraday's and Ampere's laws are implemented on an array of electrically small spatially orthogonal contour [39]. The contours mesh in the manner of links in a chain providing a geometrical interpretation of the coupling of the two laws.

Though the FDTD algorithm has elegance and simplicity, it is computationally intensive, due to the algorithm complexity and the number of calculations required for each time step. Typically, a unit cell of the FDTD mesh has dimensions of 1/20th to 1/10th of the smallest free space wavelength in the problem domain. Thus the program memory requirements are proportional to n^3 where n is the length of each grid dimension. A constraint is also placed in the time domain such that the largest time step Δt for numerical stability satisfy the Courant condition and Δt, which is proportional to n. A combination of these conditions scales the runtime of the FDTD method by a factor of n^4 using the conventional approach.

To alleviate these limitations, several counter measures have been proposed. One approach is the time-domain diakoptics method [3, 35]; where proper modes have to be chosen carefully and the other more popular method involves parallel computing [23, 37]. Access to large computer resources does not however guarantee the validity of the numerical results computed via FDTD, or any numerical model. It is well known that one of the main disadvantages of the conventional FDTD is that it has poor numerical-dispersion properties [29]. This implies a higher spatial sampling per wavelength, especially for electrically large problems. Some of the solutions use higher-order finite-difference schemes [12, 14, 15, 30, 38]. However, these methods often have difficulties in modeling general media configurations.

As stated above, time domain methods applied to certain transient applications can be however terminated at any point of time. Likewise, the transient response generated by short duration excitations might

be prominent only on a small portion of the computation region. It is not economical to compute over the entire domain using a prohibitively small grid size and it is advisable to use appropriate basis functions to model the region of space. A promising approach to this problem is the *Multiresolution Time Domain* (MRTD) method [14]. This technique uses a wavelet and scaling function discretization of Maxwell's equations to model electromagnetic phenomenon. The wavelet and scaling functions together form a complete function space in which the electromagnetic fields can be represented. The spatial derivative operator in wavelet basis in the MRTD analysis is completely determined by a set of stencil coefficients. These stencil coefficients play a role in MRTD schemes, which is identical to the role played by centered finite differences coefficients used in the FDTD methods. Depending on the type of wavelets used, different methods are possible for evaluating the stencil coefficients. For spline wavelets, the basis functions have a polynomial representation; therefore, derivatives can be evaluated analytically [9]. The disadvantage with these wavelets is that they are not orthogonal. For interpolets [6], the wavelet basis functions are chosen such that they interpolate the function at grid points and a variant of this is the Sparse Point Representation. For this class, derivatives are evaluated by differentiating the local polynomial, in a manner similar to finite differences [19]. For the Orthogonal Wavelets, for non-standard form, Beylkin and co-workers [4] have demonstrated an efficient method for obtaining the derivative of a function represented in an orthogonal wavelet basis by a pyramid algorithm which is similar to the algorithms used generally for wavelet transforms and is based on a non-standard representation of the wavelet coefficients. The use of two sets of bi-orthogonal wavelets makes it possible to evaluate the derivative of a function given its components with respect to one basis, by evaluating the projections with respect to the other set [33]. Lastly, wavelets have been used for grid adaptation while the derivatives are calculated by finite differences [13].

The Battle Lemarie functions were the earliest to be used due to its less dispersion characteristics compared to the conventional space discrete methods [34]. The shifted interpolated properties of the Daubechies have been utilized to accommodate local meshing of the field and have shown to increase the versatility of the analysis [19]. The bi-orthogonal Cohen Daubechies Feauveau wavelets have been used recently for scattering problems [33].

From a signal processing perspective, wavelets are closely connected to filter banks. Special properties can be built in both the frequency and time domains by choosing or constructing the scaling

and wavelet function from the basic filter itself. For example they can be constructed to have useful mathematical properties such as orthogonality and normality, in order to take advantage of the extensive framework of well-developed mathematical operational techniques.

In the present work we report and outline the construction and development of a wavelet basis from the impulse response of a half band filter using a Kaiser window in the MRTD formulation. A FIR (finite impulse response) filter is used to get a linear phase simplifying the filter design process. In this, a stable filter derived by a cepstral [9] procedure which is used to calculate a set of stencil coefficients akin to the Daubechies stencil coefficients for their use in MRTD formulation. The accuracy of the computations is checked with the MRTD method using Daubechies basis reported and also comparing their performances with the analytical results, for a cavity bounded with metallic walls.

In sections to follow, the basic MRTD scheme, construction and development of a set of stencil coefficients using a filter approach from filter banks, establishment of their use in the MRTD technique are presented. This is followed by validation of the results using the calculated stencil coefficients in a typical one and two dimensional MRTD scheme and comparing with the reported Daubechies based MRTD results as well those obtained through an analytical computation.

2. THE MRTD ALGORITHM

The MRTD approach as used and described in this work retains the philosophy of the original leapfrog algorithm employed in the conventional FDTD algorithm. The magnetic field components are shifted by half a discretization interval in space and time domain with respect to the electric fields. The arrangement of the electric and magnetic fields is explained, expanding on the formulation provided in [9].

2.1. Field Expansion and Meshing

The notion of the equivalent MRTD grid points in any one dimension is as follows Consider an rth order MRTD scheme. Then the use of $r+1$ wavelet levels enhances the resolution of the scheme with respect to its scaling function only based counterpart by a factor of $\rho = 2^{r+1}$, rendering the effective size of the method equal to $\Delta_r = \Delta/\rho$. Hence, within a scaling level, extending from $x_n = n\Delta$ to $x_{n+1} = (n+1)\Delta$, the equivalent grid points that are introduced by a multiresolution

expansion

$$x_n^p = (p + 1/2)\Delta_r$$
$$p = 0, 1, \ldots, 2^{r+1} - 1.$$

To determine the shift between electric and magnetic field nodes (which in FDTD is equal to 0.5) in an arbitrary order wavelet scheme, the condition $s = s_r = \Delta r/2$ is imposed. Then the field expansions read as

$$E(x,t) = \sum_n h_n(t) \sum_j \left\{ {}_nE_j^{\phi}\phi_j(x) + \sum_{r,p} {}_nE_j^{r,p}\psi_{j,p}^r(x) \right\} \quad (1)$$

$$H(x,t) = \sum_n h_{n+0.5}(t) \sum_j \left\{ {}_{n+0.5}H_{j+s_r}^{\phi}\phi_{j+s_r}(x) + \sum_{r,p} {}_{n+0.5}H_{j+0s_r}^{r,p}\psi_{j+s_r,p}^r(x) \right\} \quad (2)$$

where h_n are pulse functions in time, and $\phi_j(x)$, $\psi_{j,p}^r(x)$ represents the scaling and r-resolution wavelet function respectively. The indices j and n are the discrete space and time indexes related to the space and time co-ordinates via $x = j\Delta x$ and $t = n\Delta t$, where Δx and Δt are the space and time discretization intervals respectively.

2.2. Field Update Equations

To derive the update equations, the Method of Moments is applied to discretize the Maxwell's equation in the sense of [14]. Upon inserting the expansions, Maxwell's equations are sampled using pulse functions as time domain test functions and scaling/wavelet functions as space domain test functions. To this purpose, integrals of the generic form:

$$\int_{-\infty}^{+\infty} \frac{dg_{n\pm s_r}(x)}{dx} f_n(x)dx \quad (3)$$

with $g,\ f = \phi, \psi_p^r$. These are evaluated using any one of the techniques [4, 19, 34] mentioned in Section 1 depending upon the type of wavelet used. In the simple FDTD algorithm these are represented by the weighted sums representing the scaling-scaling, scaling-wavelet

and wavelet-wavelet interactions represented by

$$a = \int_{-\infty}^{+\infty} \frac{d\phi_{n\pm s_\gamma}(x)}{dx}\phi_n(x)dx \qquad b = \int_{-\infty}^{+\infty} \frac{d\psi_{n\pm s_r}(x)}{dx}\psi_n(x)dx$$
$$c = \int_{-\infty}^{+\infty} \frac{d\phi_{n\pm s_\gamma}(x)}{dx}\psi_n(x)dx \qquad d = \int_{-\infty}^{+\infty} \frac{d\psi_{n\pm s_r}(x)}{dx}\phi_n(x)dx$$

This leads to the update form for the 2-D TM mode [33, 34], as given by equations.

$$\begin{aligned}
H^{\phi}_{k,m} =& H^{\phi}_{k-1,m} + \frac{\Delta t}{\mu\Delta x}\left(\sum_{i=1}^{n_a} a(i)\left(E^{\phi}_{k,m+i} - E^{\phi}_{k,m-i+1}\right)\right.\\
&\left. + \sum_{i=1}^{n_c} c(i)\left(E^{\psi}_{k,m+i} - E^{\psi}_{k,m-i}\right)\right)\\
H^{\psi}_{k,m} =& H^{\psi}_{k-1,m} + \frac{\Delta t}{\mu\Delta x}\left(\sum_{i=1}^{n_d} d(i)\left(E^{\phi}_{k,m+i} - E^{\phi}_{k,m-i}\right)\right.\\
&\left. + \sum_{i=1}^{n_b} b(i)\left(E^{\psi}_{k,m+i-1} - E^{\psi}_{k,m-i}\right)\right)\\
E^{\phi}_{k+1,m} =& E^{\phi}_{k,m} + \frac{\Delta t}{\varepsilon\Delta x}\left(\sum_{i=1}^{n_a} a(i)\left(H^{\phi}_{k,m+i-1} - H^{\phi}_{k,m-i}\right)\right.\\
&\left. + \sum_{i=1}^{n_c} c(i)\left(H^{\psi}_{k,m+i} - E^{\psi}_{k,m-i}\right)\right)\\
E^{\phi}_{k+1,m} =& E^{\psi}_{k,m} + \frac{\Delta t}{\varepsilon\Delta x}\left(\sum_{i=1}^{n_d} d(i)\left(H^{\phi}_{k,m+i} - H^{\phi}_{k,m-i}\right)\right.\\
&\left. + \sum_{i=1}^{n_b} b(i)\left(H^{\psi}_{k,m+i} - E^{\psi}_{k,m-i+1}\right)\right)
\end{aligned} \tag{4}$$

Table 3 gives typical sample results of the computations of the scaling-scaling, scaling-wavelet and wavelet-wavelet interactions represented by a, b, c and d using the Daubechies filter coefficients.

3. THE MRTD SCHEME USING THE FILTERBANK APPROACH

As already mentioned the aim of the present work is to derive a new set of stencil coefficients in terms of scaling coefficients starting from a *half band filter designed by the window method for its application in the MRTD scheme.*

Basically the derivation of the desired filter coefficients, which generates the wavelet function, is based on the design of a perfect reconstruction filter bank. This involves design of a power symmetric filter, which in turn involves for a dyadic type of multiresolution, a half band filter (an mth band filter in general) and finding its minimum phase spectral factor [20]. The methodology to design the half band filter coefficients, the procedure to derive the causal filter from the half band filter, the calculation of stencil coefficients, the scaling coefficients and its use in the MRTD method are described in the following subsections.

3.1. Construction of the Digital Filter

Broadly two types of digital filters exist and they are, the Infinite duration Impulse Response (IIR) and the Finite duration Impulse Response (FIR). The FIR filter possesses certain properties, which make them to be preferred over an IIR filter. A FIR filter is also an *all zero system and due to its finite number of samples of finite magnitude, is* always *stable.* Another feature exclusive to FIR filter is that its phase response is linear and this often simplifies the design problem as the designer only need to meet the magnitude response specifications. On the other hand, for the same stop-band attenuation, the FIR filter usually requires a longer filter length than an IIR filter requiring more computations/hardware for the implementation. The Digital Filter Design problem involves the determination of a set of filter coefficients to meet a set of design specifications. These specifications typically consist of the passband width and its gain/peak ripple tolerable, the stopband width and its minimum attenuation, the transition width determined by the band edge frequencies. Towards this end we design an ideal low pass filter in the frequency domain of the form given by:

$$U_{LP}(\omega) = \begin{cases} 1 & |\omega| \leq \omega_c \\ 0 & \text{otherwise} \end{cases} \tag{5}$$

$U_{LP}(\omega)$ is band limited, and its discrete inverse Fourier transforms $u_{LP}(n)$ is an infinite-duration impulse, defined for $-\infty < n < \infty$. In order to avoid convolution with an infinite sequence of samples, $u_{LP}(n)$

is multiplied by a window-function $w(n)$ constituted by $(M+1))$ samples. The resulting filtering sequence yields:

$$u(n) = w(n)u_{LP}(n). \tag{6}$$

In order to avoid Gibbs phenomenon, a window-function with smooth edges is used. For perfect reconstruction, the halfband filter should be an equiripple filter, which has equiripple both in the passband and the stopband. In view of this, the window to be applied should be of this nature and the Kaiser window is the only window that provides the equiripple characteristic given by

$$w(n) = \begin{cases} I_0\left(\beta/m\left[m^2-(n-m)^2\right]^{1/2}\right)\Big/ I_0(\beta) \\ \qquad\qquad 0 \le n \le M \\ 0 \qquad\qquad \text{otherwise} \end{cases} \tag{7}$$

where $I_0(.)$ is the zeroth-order modified Bessel function of the first kind, and β is a shape parameter.

For a lowpass filter characterized by stopband attenuation A (dB), normalized transition width $\Delta\omega$ and cutoff frequency ω_c, the empirical formula for the Kaiser window is given by [22]

$$\omega(n) = \begin{cases} 0.1102(A-87) & A > 50 \\ 0.5842(A-2)^{0.4} & \\ +0.7886(A-21) & 21 \le A \le 50 \\ 0.0 & A < 21 \end{cases} \tag{8a}$$

$$M = (A-8)/(2.285\Delta\omega) \tag{8b}$$

3.2. Physically Realizable Filter

A filter is said to be physically realizable if it is minimum phase. That is its impulse response $h(n)$ is causal and stable. In terms of poles and zeros, a filter is causal if and only if all its poles and zeros are inside the unit circle in the Z-plane.

For a pole outside the unit circle, the impulse response has an exponentially increasing component. The impulse response component corresponding to a pole on the unit circle results in a sustained oscillations and it neither decays nor grows. A zero outside the unit circle though does not affect the stability but results in an impulse response, which is *anti-causal*. A minimum-phase impulse response can be derived by computing the cepstrum from the magnitude spectrum [20] The cepstrum/ real cepstrum is defined as the inverse

Fourier transform (FT) of the logarithm of the magnitude spectrum. If $x(\omega)$ is the FT of $x(\omega)$, then its cepstrum is

$$\hat{x}_e(n) = F^{-1}\left[0.5 \ln\left\{|X(\omega)|\right\}\right] \tag{9a}$$

Since the cepstrum is the inverse FT of the logarithm of the spectral magnitude, it represents the even part of the original cepstrum. Since the interest is to get the minimum phase impulse response, its cepstrum corresponds to a sequence, which is weighted as below:

$$g(n) = \begin{cases} 1, & n = 0, N/2 \\ 2, & n = 1, \ldots, N/2 - 1 \\ 0, & n = N/2 + 1, \ldots, N \end{cases} \tag{9b}$$

The cepstrum of the minimum phase impulse response is

$$\hat{x}_{mp}(n) = g(n)\hat{x}_e(n) \tag{9c}$$

From the cepstrum of the impulse response, the impulse response is derived as below:

$$x_{mp}(n) = F^{-1}\left[\exp\left\{\hat{X}_{mp}(\omega)\right\}\right] \tag{9d}$$

The computed cepstral response for the designed filter is shown in Fig. 1. for the design values given in Table 1. The scaling and wavelet coefficients are next calculated from the filter coefficients and finally these are used to obtain the stencil coefficients a, b, c, and d as described in the next sub-sections.

Table 1. FIR Type I filter design values.

Sr. No.	**Parameter**	**Value**
1	N	**6, 8, 10**
2	**Cutoff frequency ω_c; $(0 < \omega_c < 1)$**	**0.5550**
3	**Beta**	**4.25, 7.1, 10.2**
4	**Filter type**	**Low-pass**

3.3. Computation of Stencil Coefficients

Based on the algorithm presented in [4, 21] the stencil coefficients can be derived analytically.

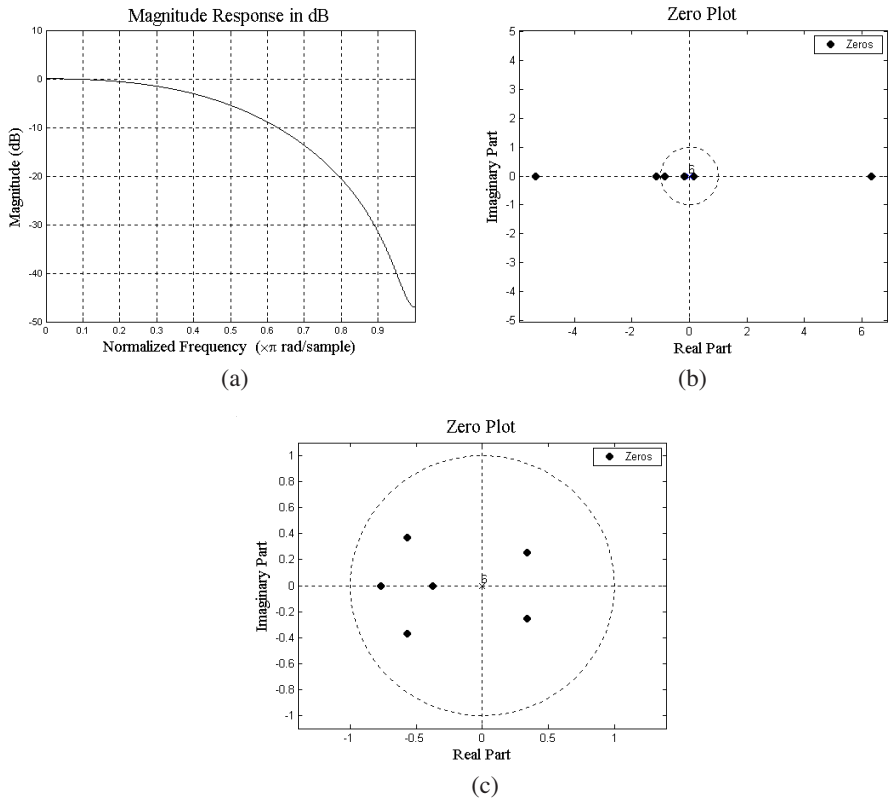

Figure 1. (a) Magnitude response, (b) zero plot before cepstral, (c) zero plot after cepstral for $N = 6$ and beta $= 4.25$, Kaiser window.

The coefficients r_l are of the form

$$r_l = \int_{-\infty}^{\infty} \phi\,(x-l)\frac{d}{dx}\phi(x)dx, \quad l \in z \tag{10}$$

The coefficients r_l vanish for $l < -2N+2$ and $l > 2N-2$. By definition,

$$r_{-l} = -r_l, \quad l \in z \tag{11}$$

and it is shown that

$$\sum_{l \in z} r_l = 0. \tag{12}$$

The coefficients $r_l$also satisfy

$$\sum_{l\in z} lr_l = -1, \tag{13}$$

$$r_l = 2r_{2l} + \sum_{k=1}^{N} \tilde{a}_{2k-1}[r_{2l-2k+1} + r_{2l+2k-1}], \tag{14}$$

where the coefficients $\tilde{a}_n$ are the autocorrelation of scaling coefficients h_i, defined as

$$\tilde{a}_k = 2 \sum_{i=0}^{2N-1-n} h_i h_{i+n}, \quad n = 1, \ldots, 2N-1 \tag{15}$$

The stencil coefficients a_p can then be computed using (15). Once the stencil coefficients are calculated the scaling coefficients are obtained using the procedure described in the next section.

3.4. Computation of Scaling Functions

The scaling function ϕ satisfies the following linear system:

$$\phi(x) = \sqrt{2} \sum_{i=0}^{2N-1} h_i \phi(2x - i), \tag{16}$$

where $\{h_i\}_{i=0,\ldots,2N-1}$ are the scaling coefficients. The support of ϕ is $[0,\ 2N-1]$, and ϕ also vanishes at the bounds of the interval, the task is to compute $\{\phi_k = \phi(k)\}_{k=1,\ldots,2N-2}$. Following the procedure outlined in [21], we use (16) to obtain the matrix equation

$$M\tilde{\phi} = \tilde{\phi} \tag{17}$$

$$[M - I]\,\tilde{\phi} = 0 \tag{18}$$

where $\tilde{\phi} = [\phi_1 \phi_2 \ldots \phi_{2N-2}]^T$. The elements of the matrix M are the scaling coefficients, which are known. Since the matrix $[M - I]$ is singular, the last row is replaced by the normalizing condition $\sum_{k\in z} \phi_k = 1$ and the resulting linear system of equations are solved for ϕ are calculated for the Daubechies wavelet and for the designed wavelet as shown in Table 2.

Table 2. Impulse response coefficients and scaling function.

Filter Order	k	Daubechies			Present Approach		
		h(k)	ϕ (k)	ψ (k)	h(k)	ϕ (k)	ψ (k)
6	1	3.3262e-1	-1.1360e-16	-5.6594e-18	4.5282e-1	0	0
	2	8.0677e-1	1.2863e+0	1.3621e-1	7.3916e-1	6.5138e-2	9.9784e-1
	3	4.5981e-1	-3.8584e-1	-7.5120e-1	3.1594e-1	-4.3607e-1	-7.0639e-2
	4	-1.3499e-1	9.5268e-2	-1.1082e+	-6.4384e-2	-7.3354e-1	5.0031e-2
	5	-8.5428e-2	4.2343e-3	-3.9988e-2	-4.7442e-2	-4.3423e-2	-8.1114e-4
	6	3.5221e-2	-1.2232e-16	5.7548e-17	1.8113e-2	-1.5101e-2	2.3581e-2
8	1	2.3034e-1	-2.0578e-16	3.0840e-18	4.4167e-1	1.0061e-16	-1.0943e-18
	2	7.1474e-1	1.0072e+0	-4.6330e-2	7.3272e-1	1.0073e+0	2.3301e-2
	3	6.3079e-1	-3.3837e-2	2.6326e-1	3.1544e-1	-5.8406e-2	2.6516e-2
	4	-2.7980e-2	3.9610e-2	-8.8724e-1	-4.0055e-2	1.5208e-2	-4.4555e-1
	5	-1.8701e-1	-1.1764e-2	-3.9754e-1	-1.8884e-2	1.4330e-2	-6.9682e-1
	6	3.0837e-2	-1.1980e-3	-2.3730e-2	6.9192e-3	-1.8238e-3	6.7677e-3
	7	3.2878e-2	1.8829e-5	4.0933e-4	-1.5911e-2	2.4099e-4	-8.9409e-3
	8	-1.0596e-2	-4.7000e-17	1.5313e-17	-7.6906e-3	2.3155e-2	-1.4463e-2
10	1	1.6008e-1	1.3548e-17	6.3913e-20	4.2067e-1	1.8735e-16	-3.9341e-19
	2	6.0374e-1	6.9614e-1	1.4504e-2	7.3016e-1	9.9705e-1	-4.3754e-3
	3	7.2420e-1	4.4906e-1	-8.3399e-2	3.3336e-1	-5.4645e-2	5.9558e-3
	4	1.3841e-1	-1.8225e-1	2.3774e-1	-3.5174e-2	1.4759e-2	4.8116e-2
	5	-2.4226e-1	3.7232e-2	-6.8946e-1	-3.3729e-2	9.2002e-3	-4.6660e-1
	6	-3.2240e-2	1.5176e-3	4.2042e-1	-5.6049e-3	1.6345e-2	-6.5629e-1
	7	7.7560e-2	-1.7268e-3	7.1180e-2	-4.6974e-3	-7.1375e-4	-6.8411e-3
	8	-6.2405e-3	3.7569e-5	-1.8566e-3	7.5298e-3	-1.8342e-4	-9.5253e-3
	9	-1.2579e-2	1.7413e-7	-8.3577e-6	3.1844e-3	1.9290e-4	-8.1762e-3
	10	3.3352e-3	-2.3634e-16	5.3512e-17	-1.4848e-3	1.7997e-2	-1.0707e-2

4. VALIDATIONS

The stencil coefficients a, b, c, d calculated using the analytical approach [4] and listed in Table 3. are used with a one and two dimension MRTD algorithm for validations. We consider the one dimension telegrapher's equations and study the cross talk behavior of a printed circuit line for the one-dimensional case and validated by the FDTD method with experimental results in [24]. The board is glass-epoxy, and the thickness is 47 mils, width are 15 mils, and the lands have a center-to-center separation of 30 mils and are 10 inches in length. The source voltage is a 10 MHz, 1 V trapezoidal pulse train with a 50% duty cycle and rise/fall times of 6.25 ns. Fig. 2 shows the near end cross talk voltages using the FDTD method, the MRTD method with Daubechies stencil coefficients as well as the MRTD method with the stencil coefficients calculated by us, using the filter approach. As can be seen there is reasonable correlation indicating the validity of the present approach.

Next, a simple air filled cavity of $2m \times 2m$ size with perfectly

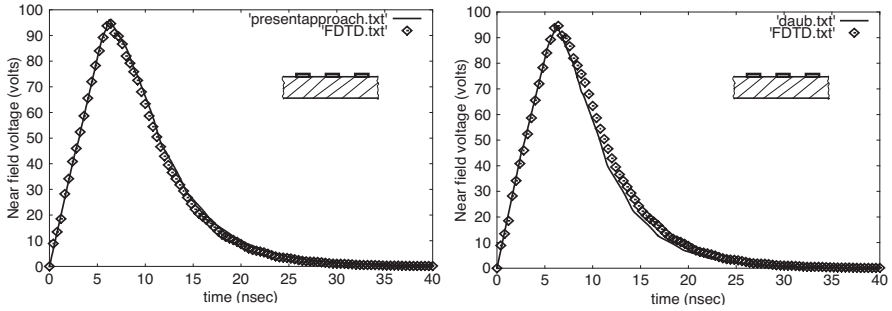

Figure 2. Performance Comparisons of the new stencil coefficients with analytical results, the FDTD method and Daubechies coefficients for the inset geometry.

Table 3. MRTD coefficients for the Daubechies-6 wavelet family and using present approach, $N = 6$.

	Index k	a	b	c	d
Daubechies	-4	-8.49e-6	8.49e-6	8.02e-5	-8.99e-7
	-3	0.0034	-0.0034	-0.0323	0.0003
	-2	-0.0287	-0 .0287	0.1003	-0.0049
	-1	0.1368	-0.1953	-0.0760	0.0444
	0	-1.2910	-1.687	-0.0555	-0.1034
	1	1.2910	1.687	0.1034	0.0555
	2	-0.1368	0.1953	-0.0446	0.0760
	3	0.0287	-0.0287	0.0049	-0.1003
	4	-0.0034	0.0034	-0.0003	0.0323
	5	8.49e-6	-8.49e-6	8.99e-7	-8.02e-5
Present Approach	-4	-3.58e-6	3.58e-6	8.95e-5	-1.43e-7
	-3	0.0016	-0.0016	-0.0358	5.91e-5
	-2	-0.0017	0.0017	0.0454	-0.0008
	-1	-0.0363	-0.0005	0.0092	0.0106
	0	-0.8943	-1.306	-0.0348	-0.0258
	1	0.8943	1.306	0.0258	0.0348
	2	0.0363	0.0005	-0.0106	-0.0092
	3	0.0017	-0.0017	0.0008	-0.0454
	4	-0.0016	0.0016	-5.91e-5	0.0358
	5	3.58e-6	-3.58e-6	1.43e-7	-8.95e-5

conducting walls, and a discretization of ten samples per wavelength is considered. The incident pulse is $s(t) = \exp[-(t - taug)/2\sigma^2]^2$ assumed to be a Gaussian current source with a time series form given by where $taug = 1.0\text{e} - 8\,\text{sec}$ and $\sigma = 1.0\text{e} - 9\,\text{sec}$. The electrical

field distribution at the end of $1.0e-8$ sec is shown in Fig. 3. These are compared with the analytical results as well as the MRTD scheme using Daubechies wavelets. As can be seen again, good agreement is obtained. The procedure is repeated for different lengths as well, and these are also found to give good co-relation with the Daubechies filter values indicating the validity of the assumptions and the calculations made. All the results are not repeated for brevity here. It may be mentioned here that although the Daubechies wavelet is used as a reference for comparison, by a proper choice of the shape parameter β it is as well possible to design other wavelet functions which are appropriate for other applications, indicating the flexibility and the versatility of the proposed design method.

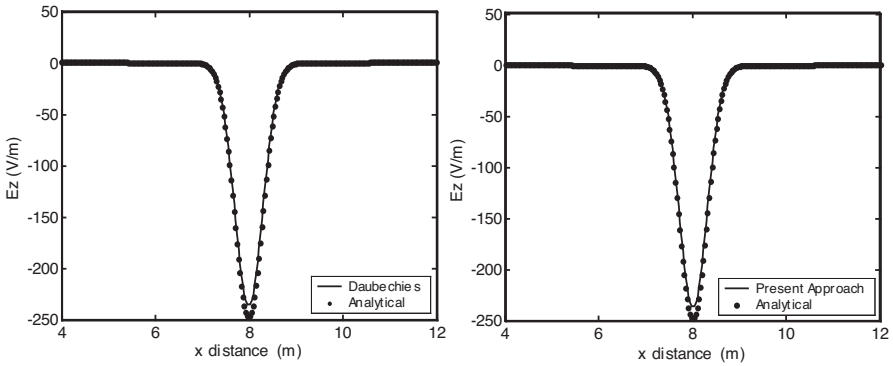

Figure 3. Performance Comparisons of the new stencil coefficients with Daubechies and the FDTD (cavity problem).

5. CONCLUSIONS

A new set of stencil coefficients in terms of scaling coefficients starting from a half band filter, designed by window method and deriving a physically realizable filter by spectral factorization using cepstral technique, for the MRTD method is presented. The new coefficients are found to give good agreement with similar MRTD schemes such as those obtained using Daubechies orthogonal wavelets. The method enables choice of wavelets by the choice of the design parameter.

REFERENCES

1. Ali, M. and S. Sanyal, "FDTD analysis of rectangular waveguide in receiving mode as EMI sensors," *Progress In Electromagnetics*

Research B, Vol. 2, 291–303, 2008.

2. Ali, M. and S. Sanyal, "FDTD analysis of dipole antenna as EMI sensor," *Progress In Electromagnetics Research*, PIER 69, 341–359, 2007.
3. Alimenti, F., P. Mezzanotte, I. Roselli, and R. Sorrentino, "Modal absorption in the FDTD method: A critical review," *International Journal of Numerical Modeling: Electronic Networks, Devices and Fields*, Vol. 10, No. 4, 245–264, July–August 1997.
4. Beylkin, G., "On the representation of operators in basis of compactly supported wavelets," *SIAM Journal on Numerical Analysis*, Vol. 29, 1716–1740, December 1992.
5. Chen, X., D. Liang, and K. Huang, "Microwave imaging of 3-D buried objects using parallel genetic algorithm combined with FDTD technique," *Journal of Electromagnetic Waves and Applications*, Vol. 20, No. 13, 1761–1774, 2006.
6. Cheong, Y., Y. M. Lee, K. H. Ra, J. G Kang, and C. C Shin, "Wavelet Galerkin scheme of time dependent inhomogeneous electromagnetic problems," *IEEE Microwave Guided Wave Lett.*, Vol. 9, 297–299, Aug. 1999.
7. Choi, S. H., D. W. Seo, and N. H. Myung, "Scattering analysis of open-ended cavity with inner object," *Journal of Electromagnetic Waves and Applications*, Vol. 21, No. 12, 1689–1702, 2007.
8. Dogaru, T. and L. Carin, "Multiresolution time domain using CDF biorthogonal wavelets," *IEEE Trans. Microwave Theory Tech.*, Vol. 49, 902–912, May 2001.
9. Tentzeris, E. M., A. Cangellaris, L. P. B. Katehi, and J. Harvey, "Multiresolution time domain (MRTD) adaptive schemes using arbitrary resolution of wavelets," *IEEE Trans. Microwave Theory Tech.*, Vol. 50, 501–513, February 2002.
10. Fayedeh, H., C. Ghobadi, and J. Nourinia, "An improvement for FDTD analysis of thin-slot problems," *Progress In Electromagnetics Research B*, Vol. 2, 15–25, 2008.
11. Golestani-Rad, L., J. Rashed-Mohassel, and M. M. Danaie, "Rigorous analysis of EM-wave penetration into a typical room using FDTD method: The transfer function concept," *Journal of Electromagnetic Waves and Applications*, Vol. 20, No. 7, 913–926, 2006.
12. Hadi, M. F. and R. K. Dib, "Phase-matching the hybrid FV24/S22 FDTD algorithm," *Progress In Electromagnetics Research*, PIER 72, 307–323, 2007.
13. Jameson, L., "On the daubechies based wavelet differentiation

matrix," Technical Report 93–95, ICASE, NASA Langley Research Center, 1993.

14. Krumphotz, M. and L. P. B. Katehi, "MRTD: New time domain schemes based on multiresolution analysis," *IEEE Trans. Microwave Theory Tech.*, Vol. 44, 555–571, April 1996.
15. Kung, F. and H.-T. Chuah, "Finite-Difference Time-Domain (FDTD) software for simulation of printed circuit board (PCB) assembly," *Progress In Electromagnetics Research*, PIER 50, 299–335, 2005.
16. Kuzu, L., V. Demir, A. Z. Elsherbeni, and E. Arvas, "Electromagnetic scattering from arbitrarily shaped chiral objects using the finite difference frequency domain method," *Progress In Electromagnetics Research*, PIER 67, 1–24, 2007.
17. Lee, J. H. and H. T. Kim, "Radar target discrimination using transient response reconstruction," *Journal of Electromagnetic Waves and Applications*, Vol. 19, 655–669, 2005.
18. Mouysset, V., P. A. Mazet, and P. Borderies, "A new approach to evaluate accurately and efficiently electromagnetic fields outside a bounded zone with time-domain volumic methods," *Journal of Electromagnetic Waves and Applications*, Vol. 20, No. 6, 803–817, 2006.
19. Fujii, M. and W. J. R. Hoefer, "Interpolating wavelet Galerkin model of time dependent inhomogeneous electrically large optical waveguide problems," *IEEE MTT-S Digest*, 1045–1048, 2001.
20. Narasimhan, S. V. and S. Veena, *Signal Processing — Principles and Implementation*, Narosa Publishers, New Delhi, India, 2005.
21. Kovvali, N., W. Lin, and L. Carin, "Accurate computation of stencil coefficients for multiresolution time domain," available at www.duke.edu/ narayan/
22. Oppenheim, A. V. and R. W Shafer, *Discrete-Time Signal Processing*, Prentice Hall, 1989.
23. Pala, W. P., A. Taflove, M. J. Piket, and R. M. Joseph, "Parallel finite difference time domain calculations," *IEEE Trans. Antennas & Propagation*, Vol. 30, 83–85, 1991.
24. Paul, C. R., "Incorporation of terminal constraints in the FDTD analysis of transmission lines," *IEEE Trans. Electromagnetic Compat.*, Vol. 36, 85–93, May 1994.
25. Petropoulos, P. G., "Phase error control for FDTD methods of second and fourth order accuracy," *IEEE Trans. Antennas & Propagation*, Vol. 42, 859–862, 1994.

26. Poljak, D. and V. Doric, "Wire antenna model for transient analysis of simple grounding systems, Part I: The vertical grounding electrode," *Progress In Electromagnetics Research*, PIER 64, 149–166, 2006.
27. Poljak, D. and V. Doric, "Wire antenna model for transient analysis of simple grounding systems, Part II: The horizontal grounding electrode," *Progress In Electromagnetics Research*, PIER 64, 167–189, 2006.
28. Roberts, T. M., "Measured electromagnetic pulses verify asymptotic and analysis for linear, dispersive media," *Journal of Electromagnetic Waves and Applications*, Vol. 20, 1845–1851, 2006.
29. Shalger, K. L., J. G. Maoloney, S. L. Ray, and A. F. Peterson, "Relative accuracy of several Finite Difference Time Domain methods in two and three dimensions," *IEEE Trans. Antennas & Propagation*, Vol. 41, 1732–1737, 1993.
30. Shao, W., B.-Z. Wang, and X.-F. Liu, "Complex variable technique in compact 2-D order-marching time-domain method," *Journal of Electromagnetic Waves and Applications*, Vol. 21, No. 11, 1453–1460, 2007.
31. Taflove, A., "Review of the formulation of the FDTD method of numerical model of electromagnetic wave interaction with arbitrary structures," *Wave Motion*, Vol. 10, 547–582, 1988.
32. Tang, M., J. F. Mao, and X. C. Li, "A novel time-domain integration method for transient analysis of non-uniform transmission lines," *PIERS Online*, Vol. 3, No. 1, 2007.
33. Dogaru, T. and L. Carin, "Scattering analysis by the multiresolution time domain method using compactly supported wavelet systems," *IEEE Trans. Antennas Propagat.*, Vol. 50, July 2002.
34. Tentzeris, E., R. Robertson, A. Cangellaris, and L. P. B. Katehi, "Space and time adapting gridding using MRTD," *IEEE MTT-S Digest*, 337–340, 1997.
35. Huang, T.-W., H. Bijan, and T. Itoh, "The implementation of time domain diakoptics in the FDTD method," *IEEE Trans. Microwave Theory Tech.*, Vol. 42, 2149–2155, Nov. 1994.
36. Uduwawala, D., M. Norgren, P. Fuks, and A. Gunawardena, "A complete FDTD simulation of a real GPR antenna system operating above lossy and dispersive grounds," *Progress In Electromagnetics Research*, PIER 50, 209–229, 2005.
37. Varadarajan, V. and R. Mittra., "Finite-Difference Time-Domain analysis using distributed computing," *IEEE Microwave and*

Guided Wave Letters, Vol. 4, 144–145, 1994.

38. Sha, W., X. Wu, and M. Chen, "A diagonal split-cell model for the high-order symplectic FDTD scheme," *PIERS Online*, Vol. 2, No. 6, 715, 2006.
39. Yee, K. S., "Numerical solution of initial boundary value problem involving Maxwell's equations in isotropic media," *IEEE Trans. Antennas Propagat.*, Vol. 14, 302–307, May 1966.
40. Yong, Z., K. R. Shao, X. W. Hu, and J. D. Lavers, "An upwind leapfrog scheme for computational electromagnetics: CL-FDTD," *Progress In Electromagnetics Research Symposium*, Hangzhou, China, August 22–26, 2005.
41. Young, J. L. and R. Adams, "Excitation and detection of waves in the FDTD analysis of N-port networks," *Progress In Electromagnetics Research*, PIER 53, 249–269, 2005.
42. Zainud-Deen, S. H., W. M. Hassen, E. M. Ali, K. H. Awadalla, and H. A. Sharshar, "Breast cancer detection using a hybrid finite difference frequency domain and particle swarm optimization techniques," *Progress In Electromagnetics Research B*, Vol. 3, 35–46, 2008.
43. Zhang, Y., W. Ding, and C. H. Liang, "Study on the optimum virtual topology for MPI based parallel conformal FDTD algorithms on PC clusters," *Journal of Electromagnetic Waves and Applications*, Vol. 19, No. 13, 1817–1831, 2005.